Trapped Electromagnetic Modes and Scaling in the Transmittance of Perforated Metal Films

S. Selcuk, K. Woo, D. B. Tanner, and A. F. Hebard
Department of Physics, University of Florida, Gainesville, Florida 32611, USA

A. G. Borisov[1] and S. V. Shabanov[2,*]
[1]*Laboratoire des Collisions Atomiques et Moléculaires, UMR CNRS-Université Paris-Sud 8625, Bâtiment 351, Université Paris-Sud, 91405 Orsay CEDEX, France*
[2]*Department of Mathematics, University of Florida, Gainesville, Florida 32611, USA*
(Received 15 May 2006; published 10 August 2006)

We describe measurements and simulations of the enhanced transmittance by subwavelength hole arrays in silver films. The array period and hole size are systematically varied to give peak transmittances at wavelengths spanning a factor of 14. The spectra coincide when scaled using the array geometry and substrate refractive index alone, thus showing no significant dependence on the dielectric function of the metal. We argue that the spectra can be explained by interference of diffractive and resonant scattering. The resonant contribution comes from electromagnetic modes trapped in the film vicinity.

DOI: 10.1103/PhysRevLett.97.067403 PACS numbers: 78.66.−w, 42.25.Bs, 42.25.Fx, 73.20.Mf

Until recently, most people believed that light would not be transmitted by a metal film perforated by a set of holes with size smaller than the light wavelength. This conviction was proven wrong when it was discovered [1] that the transmittance of a periodic array of subwavelength holes could be very high at certain wavelengths. Indeed, the transmittance is not only many times larger than what one would estimate by taking a superposition of diffractive intensities of each individual small hole in the array [2], it is several times larger than the geometric optics predictions: the fraction of the area of the film occupied by holes. The explanation of this effect remains controversial. The early experiments [1,3–5], which have been confirmed by a number of workers [6–11], were interpreted in terms of a coupling of surface plasmons of the two surfaces of the film, which occurred whenever the wave vector of the surface plasmon could match the Bragg condition for scattering by the hole array [12–14]. Competing interpretations attribute the enhanced transmittance to dynamical diffraction [15,16] and to coherent diffraction by evanescent waves on the film surface [17].

In this Letter, we present experimental and computational results for the zero-order diffraction transmittance of silver films containing square arrays of square holes and deposited on a dielectric substrate. Our experimental results show *scaling*: the spectra of films with identical open area fractions and the same film thickness superimpose well when plotted against a scaling variable $\lambda_s = \lambda/(n_d D_g)$, where λ is the vacuum wavelength, D_g the hole array period, and n_d the substrate refractive index. The scaling symmetry, when the radiation wavelength and the structure dimensions are scaled by the same factor, is an exact symmetry of Maxwell's equations for nondispersive materials. For practical metals, this symmetry is, in general, broken because of the wavelength dependence of their dielectric functions. However, the observed scaling suggests that the transmittance peaks and dips are independent of the dielectric function (or plasma frequency) of the metal as well as of the film thickness. Apart from Ohmic losses, the main transmittance features must be similar to those for the same hole arrays in thin ideal metal films because the scaling symmetry is exact for the latter. The computations, which use a full electromagnetic theory, agree well with the experiments, including the wavelengths of the peaks and zeros, the magnitude of the transmittance, and the overall line shape of the spectral features. The scaling has also been verified by additional simulations with different dimensions of the system. Our experimental and numerical results lead to the conclusion that the transmittance is predominantly determined by geometry.

Sharp drops in the transmittance at specific values of the scaling variable are typical threshold phenomena associated with opening diffractive scattering channels. The transmittance peaks are due to a resonant scattering of light via trapped electromagnetic modes defined as the eigenvalue problem solutions of Maxwell's equations with radiating boundary conditions. They can be viewed as electromagnetic fields trapped in the vicinity of the structure and slowly decaying by emitting nearly monochromatic radiation. Our conclusion that the trapped modes are indeed the scattering resonances is based on simulations, which show that the peaks of Ohmic losses in the metal match the transmittance peaks.

Our arrays are fabricated on 100 nm thick silver films that have been thermally deposited on either fused silica or zinc selenide substrates. The films are deposited at a rate of 5–10 Å/s and have a highly specular appearance, with rms roughness determined from atomic force microscopy scans to be ~60 Å. Electron beam lithography is used to pattern the hole arrays by first spin coating the film with a positive polymer resist (PMMA) and then serially exposing each array pattern, hole by hole, with the electron beam. After

exposure and development, a 500 eV argon ion beam is used to etch away the silver in each hole. The remaining PMMA is then removed in a heated and sonicated acetone rinse. The resulting pattern on the *same* Ag film comprises nine uniformly spaced square-hole arrays, each having a total area of $(0.6\ \mathrm{mm})^2$. Therefore, the film properties were identical for all arrays. For each of the three different lattice spacings $D_g = 4, 6, 8\ \mu$m used, we choose different hole sizes a so that transmittance as a function of a and D_g can be studied.

The normal-incidence transmittance was measured over the midinfrared-ultraviolet spectral range using a Perkin-Elmer model 16U grating spectrometer (0.25–3.3 μm) and a Bruker 113v Fourier spectrometer (2–22 μm). The transmittance is normalized to that of an aperture having the same area as the hole array. The angular spread of the beam used for the measurements is 1° for the grating spectrometer and 8.5° for the Fourier spectrometer. Transmittance spectra as a function of wavelength over 2.5–22 μm for nine distinct square-hole arrays are shown in Fig. 1. As indicated in the figure, each of the three sets of arrays has the same open area fraction, $f = (a/D_g)^2$ and, within the set, the array period D_g is equal to 4, 6, and 8 μm. For every D_g, $a = D_g/3$, $D_g/2$, and $2D_g/3$. Thus, a spans the range from 4/3 to 16/3 μm. As f increases from 0.11 to 0.44, the transmittance amplitude increases significantly. As D_g increases, the transmittance peaks move to longer wavelength. For fixed D_g, the data of Fig. 1 do not reveal any systematic shift of the transmittance peaks with hole size.

The sharp drops in transmittance on the short-wavelength side of each peak are typical threshold phenomena. If the xy plane is parallel to the film and $k_{x,y,z}$ are components of the wave vector of the transmitted wave, then the periodic boundary conditions require that $k_{x,y} = k_g l_{x,y}$, where $l_{x,y}$ are integers and $k_g = 2\pi/D_g$ is the reciprocal lattice vector. For normal incidence, the incoming wave vector has only a z component of magnitude $k = 2\pi/\lambda$. Since the incoming and transmitted waves have the same frequency, one obtains

$$2\pi n_d/\lambda = \sqrt{k_g^2(l_x^2 + l_y^2) + k_z^2}. \quad (1)$$

Hence, for $\lambda_s = \lambda/(n_d D_g) > 1$ only normal transmission is possible. The diffraction thresholds are at $\lambda_s = (l_x^2 + l_y^2)^{-1/2}$. Each time λ_s becomes less than 1, $1/\sqrt{2}$, etc., for the incoming radiation, the transmittance drops as the energy leaks into new off-axis diffractive channels. The color-coded vertical dashed lines in Fig. 1 correspond to $\lambda_s = 1$ for the corresponding arrays.

Figure 2 shows the transmittance of five arrays, all with $f = 0.25$. Two (upper panel) were fabricated on fused silica and three (lower panel) on ZnSe substrates. To obtain wide wavelength coverage, we have used fused silica substrates ($n_d = 1.4$) for smaller period ($D_g = 1$ and 2 μm) hole arrays and ZnSe substrates ($n_d = 2.4$) for longer period ($D_g = 4$, 6, and 8 μm) arrays. The 70 nm thick Ag film on the fused silica substrate is thinner than the 100 nm thick Ag film on the ZnSe substrate. The first ($\lambda_s = 1$) and second ($\lambda_s = 1/\sqrt{2}$) diffraction thresholds are shown as vertical dashed lines in the figure. For each substrate, most of the spectral features scale well with λ_s, confirming, within the accuracy of the experiment, that they are determined by the film geometry. We note that for the ZnSe substrate the scaling holds for a variation in D_g (or λ) by a factor of 8.

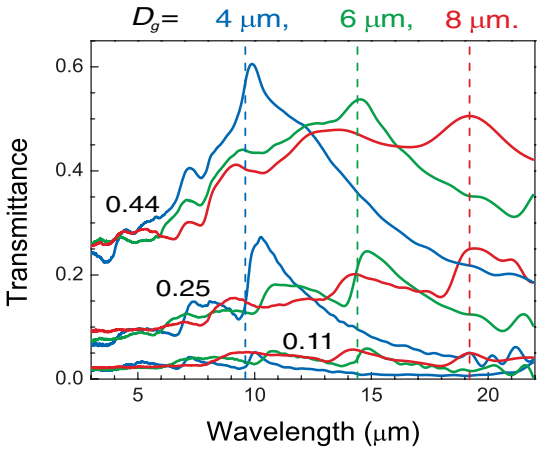

FIG. 1 (color). Transmittance vs wavelength for 9 different hole arrays. The open area fractions are 0.44 for the top 3 curves, 0.25 for the middle 3, and 0.11 for the bottom 3. The colors indicate the period: blue has $D_g = 4$ μm, green 6 μm, and red 8 μm. The number above each set of curves is the open area fraction f.

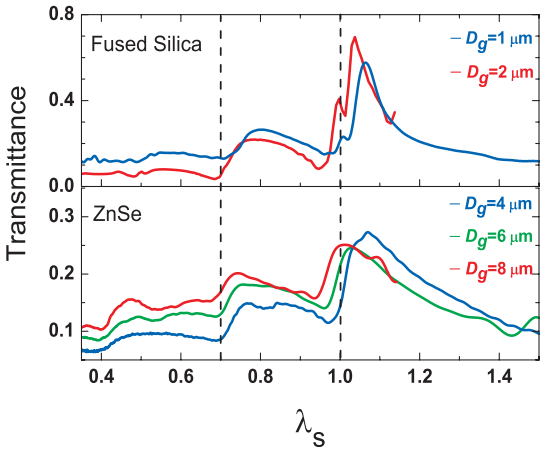

FIG. 2 (color). Transmittance vs scaling variable, $\lambda_s = \lambda/(n_d D_g)$, for five arrays with the same open area fraction, $f = 0.25$. The upper panel shows the data for two arrays made on a fused silica substrate ($n_d = 1.4$) with $D_g = 1$ μm (blue curve) and $D_g = 2$ μm (red curve). The lower panel shows the data for three arrays on ZnSe ($n_d = 2.4$). Variations in D_g and n_d yield a variation of λ by a factor of 14.

The transmittance peak positions are often explained by an enhanced coherent radiation of the holes mediated by surface plasmons. For a single planar metal-dielectric interface the plasmon dispersion relation is $k_{sp} = (\omega/c) \times [\varepsilon_d \varepsilon_m/(\varepsilon_d + \varepsilon_m)]^{1/2}$, where $\varepsilon_d = n_d^2$ and ε_m is the metal-dielectric function [18]. For *normal* incidence, the wave vector of allowed surface waves is $k_{sp} = k_g(l_x^2 + l_y^2)^{1/2}$. Because $-\mathrm{Re}\varepsilon_m \gg \varepsilon_d$, the plasmon modes are close to the diffraction thresholds and the enhanced transmittance could be attributed to a resonant scattering of light via these modes. This picture has several shortcomings. The quantization of plasmon states alone does not account for the actual array geometry. Larger values of f mean a stronger coupling between the surface wave modes at the two interfaces, and the dispersion relation has to be modified accordingly [18]. As our experiments and experiments of others [8] indicate, the transmittance does not change if the film is illuminated from either the dielectric or the vacuum side, implying that the transmittance mechanism cannot involve just a particular surface mode at either interface. Finally, it is worth mentioning that plasmons do not exist for ideal metals. Nevertheless, a 100% transmittance at λ_s slightly larger than 1 has been shown to exist in calculations for perfect metals [19]. A similar phenomenon also occurs for nondispersive dielectric gratings [20–22].

To elucidate the origin of the transmittance peaks, we have carried out numerical simulations based on the full Maxwell's theory. A time-domain Lanczos-split spectral algorithm with automatic accuracy control has been used in combination with a mapped Fourier grid spectral method [22]. A Drude model, with parameters for Ag, is used to describe the metal [23]. The results for $a = 2D_g/3$, $D_g/2$, and $D_g/3$ are shown in Fig. 3. The peak positions and overall spectral structure are in a good agreement with the experimental data. The peaks of the computed transmittance become *redshifted* and broader as f increases. The redshift appears to be hard to resolve experimentally because of imperfections in the sample geometry that lead to broadening of the experimentally observed peaks. The sharp drops of the transmittance on the short-wavelength side of the peaks are in agreement with the diffraction thresholds. To verify the scaling, we have carried out additional numerical simulations for Ag films on the ZnSe substrate with $f = 0.25$ ($D_g = 2a$, $a = 2$ and 4 μm) and the film thickness being 90 and 180 nm. For the zero-order transmittance peak position, its width, and its amplitude, the results show no difference with the black curve for $f = 0.25$ in Fig. 3, thus confirming the scaling.

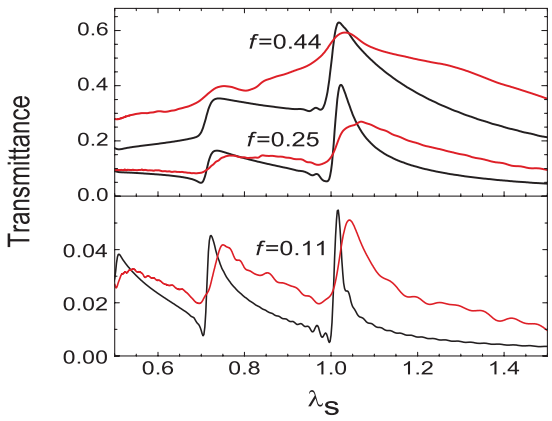

FIG. 3 (color). Comparison of numerical results (black curves) with the experiment (red curves) for three arrays with $D_g = 4$ μm.

The presence of the well-defined peaks, particularly for small f, indicates the resonant nature of the scattering process. The resonant scattering occurs through quasistationary states viewed here as electromagnetic fields trapped in the vicinity of the film slowly decaying by emitting a monochromatic radiation during characteristic times $1/\Gamma$ with Γ being the width of the corresponding transmittance peak. Given the dielectric function $\varepsilon(\omega)$, consider fixed-frequency Maxwell's equations, where the time evolution of all fields is governed by the factor $\exp(-i\omega t)$, with the radiation boundary condition at infinite distances. In our case, all the fields behave as $\exp(\pm ikz)$ as $z \to \pm\infty$ with $k > 0$. This is an eigenvalue problem for ω. The trapped modes are eigenfields corresponding to simple eigenvalues $\omega = \omega_0 - i\Gamma$. Such eigenvalues are simple isolated poles of the corresponding Green's function. By means of the Lippmann-Schwinger formalism, it can be proved [24] that the very existence of the poles leads to the enhanced transmittance with peaks of width Γ near $\lambda = 2\pi c/\omega_0$. Two types of poles are shown to exist, those determined by material resonances (polaritons, plasmons) and those determined by the perforation geometry alone (scaling) [22].

From the width of the peaks it follows that the states that contribute to the resonant part of the spectrum must be long-lived for smaller f. If the electromagnetic fields get trapped in the vicinity of the film forming a resonant state, then the longer the state lives, the more Ohmic losses it produces in the metal. For $\lambda_s > 1$, the off-axis reflection channels are closed and the losses in the transmittance can be seen as dips in the sum of the transmittance and reflectance. The latter are shown in Fig. 4 (left panels). For small holes (the lowest panel), a dip is clearly visible, indicating substantial Ohmic losses occurring at about the same wavelength as the transmittance peak (red dashed line). For large holes, no structure at $\lambda_s > 1$ is present (upper panel), and the first diffraction threshold appears as a sharp drop indicating the opening of an off-axis diffraction channel. The right panels of Fig. 4 show the computed energy density of the trapped mode over the array unit cell in the metal-dielectric interface plane. The hole is centered in the cell. The xy asymmetry of the energy density is related to the y polarization of the incoming wave packet. For a small hole, the trapped fields extend significantly over the metal as well as into the hole itself.

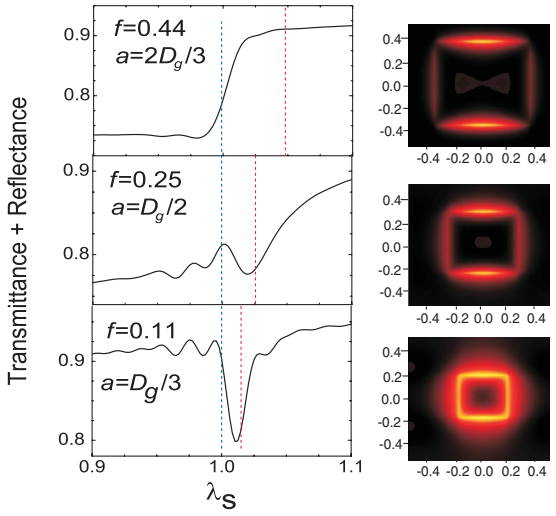

FIG. 4 (color). The sum of the calculated transmittance and reflectance (left panels) near $\lambda_s = 1$. The Ohmic losses in the metal produced by the trapped modes correspond to dips in these curves for $\lambda_s > 1$. The red dashed lines show the positions of the corresponding transmittance peaks. A redshift effect is clearly visible. The right panels show the energy density of the corresponding trapped mode in the plane of the metal-dielectric interface as a function of x/D_g (horizontal) and y/D_g (vertical). The color code varies from dark brown (zero) to bright yellow (maximum) on a linear scale.

An enhanced transmittance occurs when the normalized transmittance $T_n = T/f$ exceeds 1. If the scattering unitarity condition, $T + R = 1$, is satisfied (a lossless metal and off-axis channels closed, $\lambda_s > 1$), then, as proved in [24] for film geometries with the reflection symmetry $z \rightarrow -z$, it is always true that $T = 1$ near the resonance and, hence, $T_n = 1/f > 1$. Thus, one would expect a higher enhancement for smaller f's. However, for realistic metal films on substrates, the reflection symmetry is broken and there are two effects that decrease the enhanced transmittance. First, more reflective substrates (higher n_d) tend to suppress the measured transmittance T. Second, as f decreases, the lifetime of the trapped mode and the Ohmic losses increase (Figs. 3 and 4) so that the trapped mode dumps a substantial part of its energy into heat rather than into the far field. The calculation result shown in the lower panel of Fig. 3 for the peak at $\lambda_s > 1$ gives $T_n = 0.5$, while, without the substrate, $T_n = 3.6$. If, in addition, the Ag attenuation is set to zero, $T_n = 1/f = 9.1$. The corresponding simulation results are not shown here. The effect of the substrate is quite visible in the experimental data of Fig. 2. For the fused silica substrate, the largest $T_n = 2.8$ (red peak), while for ZnSe, $T_n = 1.1$ (blue peak).

In summary, we have shown that the transmittance of subwavelength hole arrays in metal films exhibits scaling, which is interpreted as the independence of the transmittance on the metal dispersive properties and the film thickness in the studied frequency range. The structure of the transmittance spectra is mostly determined by the perforation geometry and can be viewed as the result of interference of diffractive and resonant scattering. The transmittance minima are shown to be a threshold phenomenon associated with diffractive scattering channels determined by the array period and the substrate dielectric constant. The transmittance peaks are associated with the resonant scattering via trapped electromagnetic modes whose existence and structure is a predominantly geometric effect. As the open area fraction of the film increases, the trapped modes become short lived and the diffractive scattering mechanism dominates.

S. S., K. W., D. B. T., and A. F. H. acknowledge support by DARPA Contract No. ARO-W911NF-04-C-1236 and by Raytheon, Inc. S. V. S. is grateful to LCAM for the warm hospitality and to V. Sidis for support of this project. The authors appreciate the technical assistance by I. Kravchenko of the University of Florida Nanofabrication Facility (UFNF) and discussions with P. H. Holloway (UF) and J. P. Gayacq (LCAM).

*Corresponding author.
Electronic address: shabanov@phys.ufl.edu

[1] T. W. Ebbesen *et al.*, Nature (London) **391**, 667 (1998).
[2] H. A. Bethe, Phys. Rev. **66**, 163 (1944).
[3] H. F. Ghaemi *et al.*, Phys. Rev. B **58**, 6779 (1998).
[4] T. J. Kim *et al.*, Opt. Lett. **24**, 256 (1999).
[5] T. Thio *et al.*, J. Opt. Soc. Am. B **16**, 1743 (1999).
[6] D. E. Grupp *et al.*, Appl. Phys. Lett. **77**, 1569 (2000).
[7] Y.-H. Ye and Jia-Yu Zhang, Appl. Phys. Lett. **84**, 2977 (2004).
[8] W. L. Barnes *et al.*, Phys. Rev. Lett. **92**, 107401 (2004).
[9] R. Gordon *et al.*, Phys. Rev. Lett. **92**, 037401 (2004).
[10] K. J. K. Koerkamp *et al.*, Phys. Rev. Lett. **92**, 183901 (2004).
[11] F. Miyamaru and M. Hangyo, Phys. Rev. B **71**, 165408 (2005).
[12] F. J. Garcia-Vidal and L. Martin-Moreno, Phys. Rev. B **66**, 155412 (2002).
[13] J. A. Porto, F. J. Garcia-Vidal, and J. B. Pendry, Phys. Rev. Lett. **83**, 2845 (1999).
[14] W. L. Barnes, A. Dereux, and T. W. Ebbesen, Nature (London) **424**, 824 (2003).
[15] M. M. J. Treacy, Phys. Rev. B **66**, 195105 (2002).
[16] M. M. J. Treacy, Appl. Phys. Lett. **75**, 606 (1999).
[17] H. J. Lezec and T. Thio, Opt. Express **12**, 3629 (2004).
[18] A. V. Zayats, I. I. Smolyaninov, and A. A. Maradudin, Phys. Rep. **408**, 131 (2005).
[19] F. J. Garcia de Abajo, R. Gómez-Medina, and J. J. Sáenz, Phys. Rev. E **72**, 016608 (2005).
[20] R. Magnusson and S. S. Wang, Appl. Phys. Lett. **61**, 1022 (1992).
[21] K. Koshino, Phys. Rev. B **67**, 165213 (2003).
[22] A. G. Borisov and S. V. Shabanov, J. Comput. Phys. **209**, 643 (2005).
[23] M. A. Ordal *et al.*, Appl. Opt. **22**, 1099 (1983).
[24] A. G. Borisov, F. J. Garcia de Abajo, and S. V. Shabanov, Phys. Rev. B **71**, 075408 (2005).